Title

CD4+ T Cell NRF2 Signaling Improves Liver Transplantation Outcomes by Modulating T Cell Activation and Differentiation.

Journal

Antioxidants and Redox Signaling, 38(7-9)

Authors

Kojima, Hidenobu
Kadono, Kentaro
Hirao, Hirofumi
et al.

Publication Date

2023-03-01

DOI

10.1089/ars.2022.0094

Peer reviewed

ANTIOXIDANTS & REDOX SIGNALING
Volume 38, Numbers 7–9, 2023

DOI: 10.1089/ars.2022.0094

FORUM REVIEW ARTICLE

CD4$^+$ T Cell NRF2 Signaling Improves Liver Transplantation Outcomes by Modulating T Cell Activation and Differentiation

Hidenobu Kojima,* Kentaro Kadono,* Hirofumi Hirao, Kenneth J. Dery, and Jerzy W. Kupiec-Weglinski

Abstract

Aims: Innate and adaptive immune responses regulate hepatic ischemia–reperfusion injury (IRI) in orthotopic liver transplantation (OLT). While the mechanism of how nuclear factor erythroid 2-related factor 2 (NRF2) plays a role in liver IRI has been studied, the contribution of T cell-specific NRF2 in OLT remains unknown. In the current translational study, we investigated whether and how CD4$^+$ T cell-specific NRF2 signaling affects liver transplant outcomes in mice and humans.

Results: In the experimental arm, cold-stored (4°C/18 h) wild-type (WT) mouse livers transplanted to NRF2-deficient (NRF2-knockout [NRF2-KO]) recipients experienced greater hepatocellular damage than those in Nrf2-proficient (WT) counterparts, evidenced by Suzuki's histological scores, frequency of TdT-mediated dUTP nick end labeling (TUNEL)$^+$ cells, and elevated serum aspartate aminotransferase/alanine aminotransferase (AST/ALT) levels. *In vitro* studies showed that NRF2 signaling suppressed CD4$^+$ T cell differentiation to a proinflammatory phenotype (Th1, Th17) while promoting the regulatory (Foxp3$^+$) T cell lineage. Furthermore, OLT injury deteriorated in immune-compromised RAG2-KO test recipients repopulated with CD4$^+$ T cells from NRF2-KO compared with WT donor mice. In the clinical arm of 45 human liver transplant patients, the perioperative increase of NRF2 expression in donor livers negatively regulated innate and adaptive immune activation, resulting in reduced hepatocellular injury in NRF2-proficient OLT.

Innovation and Conclusion: CD4$^+$ T cell population expressing NRF2 attenuated ischemia and reperfusion (IR)-triggered hepatocellular damage in a clinically relevant mouse model of extended donor liver cold storage, followed by OLT, whereas the perioperative increase of NRF2 expression reduced hepatic injury in human liver transplant recipients. Thus, CD4$^+$ T cell NRF2 may be a novel cytoprotective sentinel against IR stress in OLT recipients. *Antioxid. Redox Signal.* 38, 670–683.

Keywords: NRF2, liver ischemia–reperfusion injury, liver transplantation, T cell differentiation, translational research

Introduction

THE NUCLEAR FACTOR erythroid 2-related factor 2 (NRF2) is a critical transcription factor that regulates cellular resistance to oxidants. Besides regulating phase I, II, and III drug-metabolizing enzymes, NRF2 controls NADPH production, glutathione (GSH), and thioredoxin (TXN)-based antioxidant system (Hayes and Dinkova-Kostova, 2014). Indeed, by regulating heme, iron, and lipid metabolism, NRF2 represents the cellular defense mechanism against xenobiotic and oxidative stress by expressing numerous antioxidant and detoxification genes (Tonelli et al, 2018). In addition to antioxidant responses, NRF2 is involved in cellular processes such as mitochondrial bioenergetics, stem cell quiescence, and cell death (Galicia-Moreno et al, 2020; Tonelli et al, 2018). With an emerging regulatory role of oxidative stress in cell metabolism, tumor suppression, and cell death, such as autophagy and ferroptosis, there is a significant

The Dumont-UCLA Transplantation Center, Department of Surgery, Division of Liver and Pancreas Transplantation, David Geffen School of Medicine at UCLA, Los Angeles, California, USA.
*Both these authors contributed equally to this work.

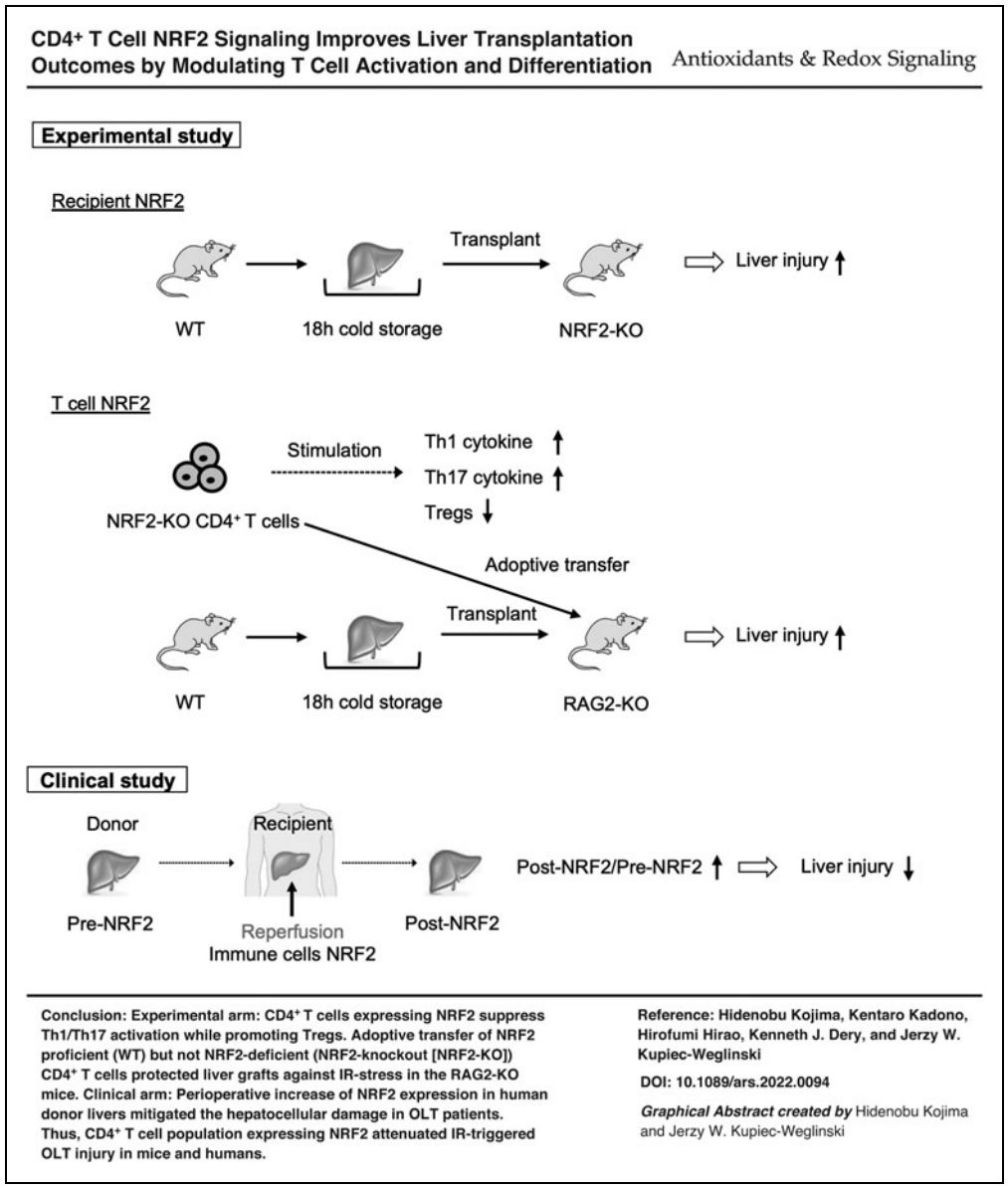

Innovation

Although the antioxidative potential of nuclear factor erythroid 2-related factor 2 (NRF2) signaling has been established, the contribution of $CD4^+$ T cell NRF2 in innate immune-driven ischemia and reperfusion (IR) stress in liver transplant recipients remains unknown. In this study, we demonstrate that $CD4^+$ T cell NRF2 signaling attenuated the peritransplant hepatocellular injury in mouse orthotopic liver transplantation (OLT) models and suppressed $CD4^+$ T cell differentiation into the proinflammatory phenotype while promoting the regulatory T cells (Tregs) *in vitro*. In parallel clinical screenings, host NRF2 immune cells mitigated hepatocellular damage in human OLT recipients. This translational study identifies $CD4^+$ T cell NRF2 as a novel therapeutic target to mitigate IR stress in liver transplantation.

interest in NRF2 as a novel checkpoint for oxidative stress responses (Chen et al, 2018).

The regulation of reactive oxygen species by NRF2 is deeply rooted in organ ischemia–reperfusion injury (IRI), a peritransplant event affecting early and late liver transplant outcomes. Hepatic ischemia and reperfusion (IR) stress occurs in two major types, with the ''cold'' IRI, initiated by liver sinusoidal endothelial cells (LSECs) injury during low-temperature donor organ preservation, followed by ''warm'' IR insult that occurs during the surgery and after graft reperfusion (Zhai et al, 2013). While the target cells and mechanisms may be distinct, NRF2 signaling was documented to regulate oxidative stress and endoplasmic reticulum stress induced by cold and warm IR insult (Cong et al, 2018; Guo et al, 2022).

Since 2013 when our group first described the hepatoprotective role of NRF2, we have reported how NRF2 signaling may regulate liver IRI (Huang et al, 2014a; Huang et al, 2014b; Ke et al, 2013; Zhang et al, 2017). Thus, the hepatocyte KEAP1-NRF2 complex has proven critical in preventing oxidative injury in the mouse orthotopic liver transplantation

(OLT) model (Ke et al, 2013), while the NRF2-HO-1 axis regulated Notch1 signaling to mediate macrophage activation and inhibit liver IRI (Huang et al, 2014a). While NRF2 activation triggered PI3K-Akt and inhibited the Foxo1 pathway in IR inflammation (Huang et al, 2014b), targeting endothelial selectins mitigated liver injury by imposing cytoprotection on LSECs in an NRF2-dependent manner (Zhang et al, 2017). Thus, various mechanisms and cell types might be involved in the NRF2 regulation of hepatic IRI.

Innate, immune-dominated, antigen-independent sterile inflammation following reperfusion is known to drive liver IRI. IR-induced cell injury produces danger-associated molecular patterns (DAMPs), which in turn activate pattern recognition receptors (PRRs), such as Toll-like receptor 4 (TLR4), to initiate an inflammatory immune cascade (Tsung et al, 2005; Zhai et al, 2004). While inhibition of innate immunity can control liver IRI, T cells are also involved in the pathogenesis of hepatic IRI (Rao et al, 2014). Indeed, we and others have documented the role of $CD4^+$ T cell-dependent adaptive immune responses, especially under cold preservation in mouse OLT recipients (Kageyama et al, 2021; Liu et al, 2015).

In the context of adaptive immunity, NRF2 is a notable molecule that elicits the anti-inflammatory function of T cells (Suzuki et al, 2020). NRF2 can suppress Th1 cytokines, such as IL-2 and IFNγ, increase IL-4, IL-5, and IL-13 production by Th2 cells, and inhibit the differentiation of proinflammatory Th17 cells (Rockwell et al, 2012; Turley et al, 2015; Zhao et al, 2016). Indeed, T cell-specific augmentation of NRF2 signaling has led to a higher frequency of $CD25^+Foxp3^+$ regulatory T cells (Tregs) and protection against IR-induced acute kidney injury (Noel et al, 2015). Thus, there is growing evidence that NRF2 works as an antioxidant molecule and may also regulate T cell differentiation. However, the contribution of T cell-specific NRF2 in liver IRI-OLT remains unknown.

In the present translational study, we used a clinically relevant mouse OLT model, well-defined cell culture systems, and human liver transplant biopsies to investigate whether and how $CD4^+$ T cell NRF2 signaling can affect IR-stressed liver transplants in mice and humans.

Results

Recipient NRF2 signaling mitigates the hepatocellular injury in IR-stressed mouse OLT

First, we used NRF2-deficient (NRF2-knockout [NRF2-KO]) mice as recipients of wild-type (WT) liver grafts in a clinically relevant model with extended donor organ cold storage, which mimics the marginal human OLT setting (Kageyama et al, 2018a). At 6 h after reperfusion, IR-triggered OLT damage, assessed by Suzuki's histological score (sinusoidal congestion, hepatocellular vacuolization, and necrosis), was significantly higher in NRF2-KO compared with WT recipients (NRF2-KO 6.7 ± 0.6 *vs*. WT 4.8 ± 0.6, $p < 0.05$) (Fig. 1A). The frequency of $TUNEL^+$ cells was increased in NRF2-KO compared with WT counterparts (NRF2-KO 68.7 ± 4.7 cells/high-power field [HPF] *vs*. WT 46.0 ± 5.0 cells/HPF, $p < 0.01$) (Fig. 1B).

We found increased frequency of OLT-infiltrating CD68 macrophages (NRF2-KO 64.5 ± 7.0 cells/HPF *vs*. WT 42.6 ± 4.4 cells/HPF, $p < 0.05$) and Ly6G neutrophils (NRF2-KO 50.7 ± 4.1 cells/HPF *vs*. WT 37.8 ± 4.4 cells/HPF, $p = 0.060$) in NRF2-KO recipients (Fig. 1B). These results suggest that disruption of NRF2 signaling at the recipient site promoted the hepatocellular damage and proinflammatory response against IR stress in OLT.

In agreement with histological findings, serum aspartate aminotransferase (AST) and alanine aminotransferase (ALT) levels were elevated in NRF2-KO compared with WT recipients (AST: NRF2-KO 4976 ± 524 *vs*. WT 2991 ± 454, $p < 0.05$; ALT: NRF2-KO 6802 ± 1030 *vs*. WT 3542 ± 495, $p < 0.05$) (Fig. 1C), confirming that recipient NRF2 signaling was required to attenuate IR liver injury. The hepatic messenger RNA (mRNA) levels coding for IL-2 and IL-17 were significantly higher. At the same time, Foxp3 and related IL-13 expression were decreased in NRF2-KO compared with WT hosts (Fig. 1D), consistent with the possibility that enrichment of a T cell proinflammatory phenotype coincides with the disruption of NRF2 signaling in OLT recipients.

Since NRF2 expression was reported to associate with immune checkpoint regulators (Oshi et al, 2020), we further evaluated mRNA coding for T cell immunoglobulin and mucin-domain containing-3 (TIM-3), programmed death-1 (PD-1), and lymphocyte activation gene 3 (LAG3). However, their expression was comparable between WT and NRF2-KO OLT recipients (Fig. 1E).

$CD4^+$ T cell NRF2 promotes $CD4^+$ T cell differentiation into $CD4^+CD25^+Foxp3^+$ Tregs

As IR-stressed liver grafts implanted into NRF2-KO recipient mice were enriched in IL-2 and IL-17 but deficient in Foxp3 and IL-13, we next evaluated the impact of NRF2 signaling on $CD4^+$ T cell phenotype *in vitro*. The purity of spleen $CD4^+$ T cells, isolated by magnetic cell sorting, was

FIG. 1. Recipient NRF2 signaling mitigates the inflammatory response and improved hepatocellular function in IR-stressed mouse OLT. Mouse livers subjected to 18 h of cold storage were transplanted into WT or NRF2-KO mouse recipients. Liver and serum samples were analyzed 6 h after reperfusion. The sham group underwent the same procedures except for OLT. **(A)** Representative H&E staining (original magnification × 200) and Suzuki's histological grading of liver IRI. **(B)** Representative TUNEL staining and immunohistochemical staining of OLT-infiltrating $CD68^+$ and $Ly6G^+$ cells (original magnification × 400) and cell quantification/HPF. **(C)** Serum AST and ALT levels (U/L). **(D)** Quantitative RT-PCR-assisted detection of mRNA coding for IL-2, IL-17, IL-13, and Foxp3 in OLT. Data were normalized to HPRT gene expression. **(E)** Quantitative RT-PCR-assisted detection of mRNA coding for TIM-3, PD-1, and LAG3 in OLT. Data were normalized to HPRT gene expression. The *triangle* indicates the sham group, the *white circle* indicates WT recipients, and the *black square* indicates NRF2-KO recipients. Data are shown as mean ± SEM. $*p < 0.05$, $**p < 0.01$, Student's *t*-test **(A–D)**, $n = 5$–6 per group. ALT, alanine aminotransferase; AST, aspartate aminotransferase; H&E, hematoxylin and eosin; HPF, high-power field; IRI, ischemia–reperfusion injury; LAG3, lymphocyte activation gene 3; mRNA, messenger RNA; PD-1, programmed death-1; RT-PCR, reverse transcription–polymerase chain reaction; SEM, standard error of the mean; TIM-3, T cell immunoglobulin and mucin-domain containing-3; TUNEL, TdT-mediated dUTP nick end labeling.

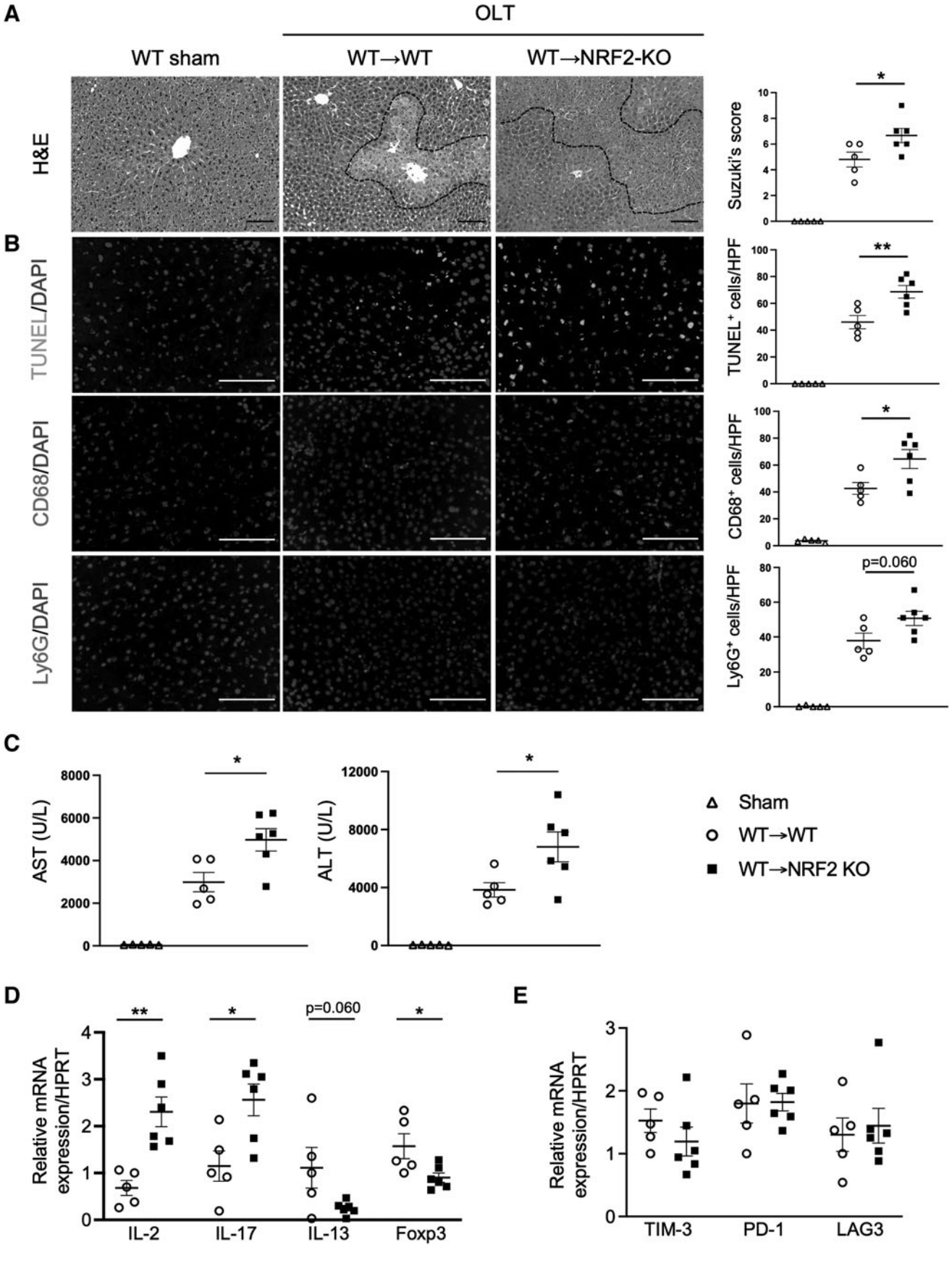
A
OLT
WT sham
WT→WT
WT→NRF2-KO
H&E
Suzuki's score
B
TUNEL/DAPI
TUNEL+ cells/HPF
CD68/DAPI
CD68+ cells/HPF
Ly6G/DAPI
Ly6G+ cells/HPF
p=0.060
C
AST (U/L)
ALT (U/L)
Sham
WT→WT
WT→NRF2 KO
D
Relative mRNA expression/HPRT
IL-2
IL-17
IL-13
Foxp3
p=0.060
E
Relative mRNA expression/HPRT
TIM-3
PD-1
LAG3

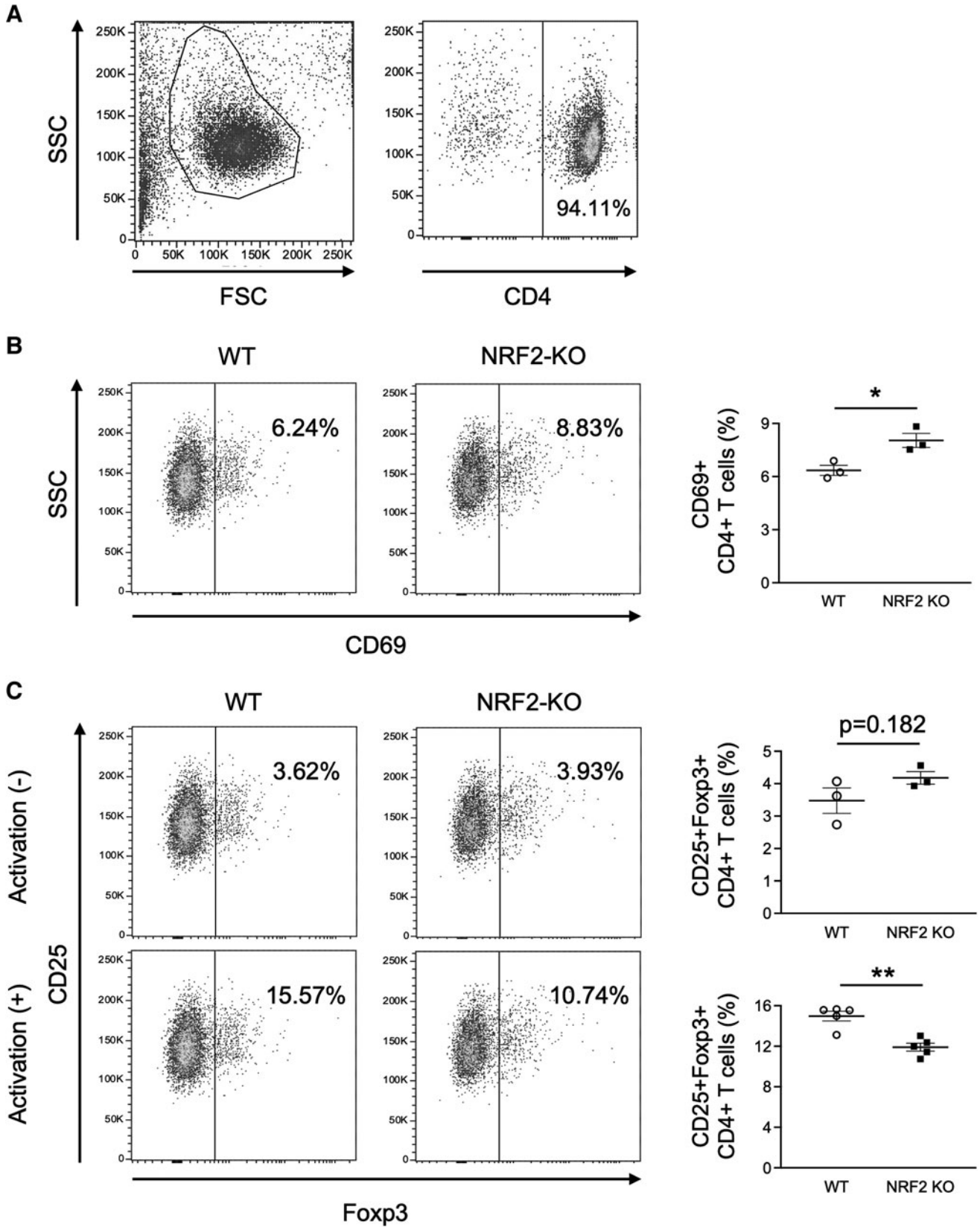

FIG. 2. $CD4^+$ T cell NRF2 signaling promotes $CD4^+$ T cell differentiation into the $CD4^+CD25^+Foxp3^+$ Tregs *in vitro*. Spleen $CD4^+$ T cells from WT and NRF2-KO mice were evaluated for $CD4^+$, $CD69^+$, CD25, and Foxp3 expression by flow cytometry. **(A)** The frequency of purified splenic $CD4^+$ T cells. **(B)** The frequency of $CD69^+$ $CD4^+$ T cells ($n = 3$ per group). **(C)** The frequency of $CD4^+CD25^+Foxp3^+$ Tregs in WT *versus* NRF2-KO mice before activation ($n = 3$ per group) and after activation with anti-CD3/CD28 antibody ($n = 5$ per group). The *white circle* indicates WT, and the *black square* indicates NRF2-deficient $CD4^+$ T cells. Data are shown as mean ± SEM **(B, C)**. $*p < 0.05$, $**p < 0.01$, Student's *t*-test **(B, C)**.

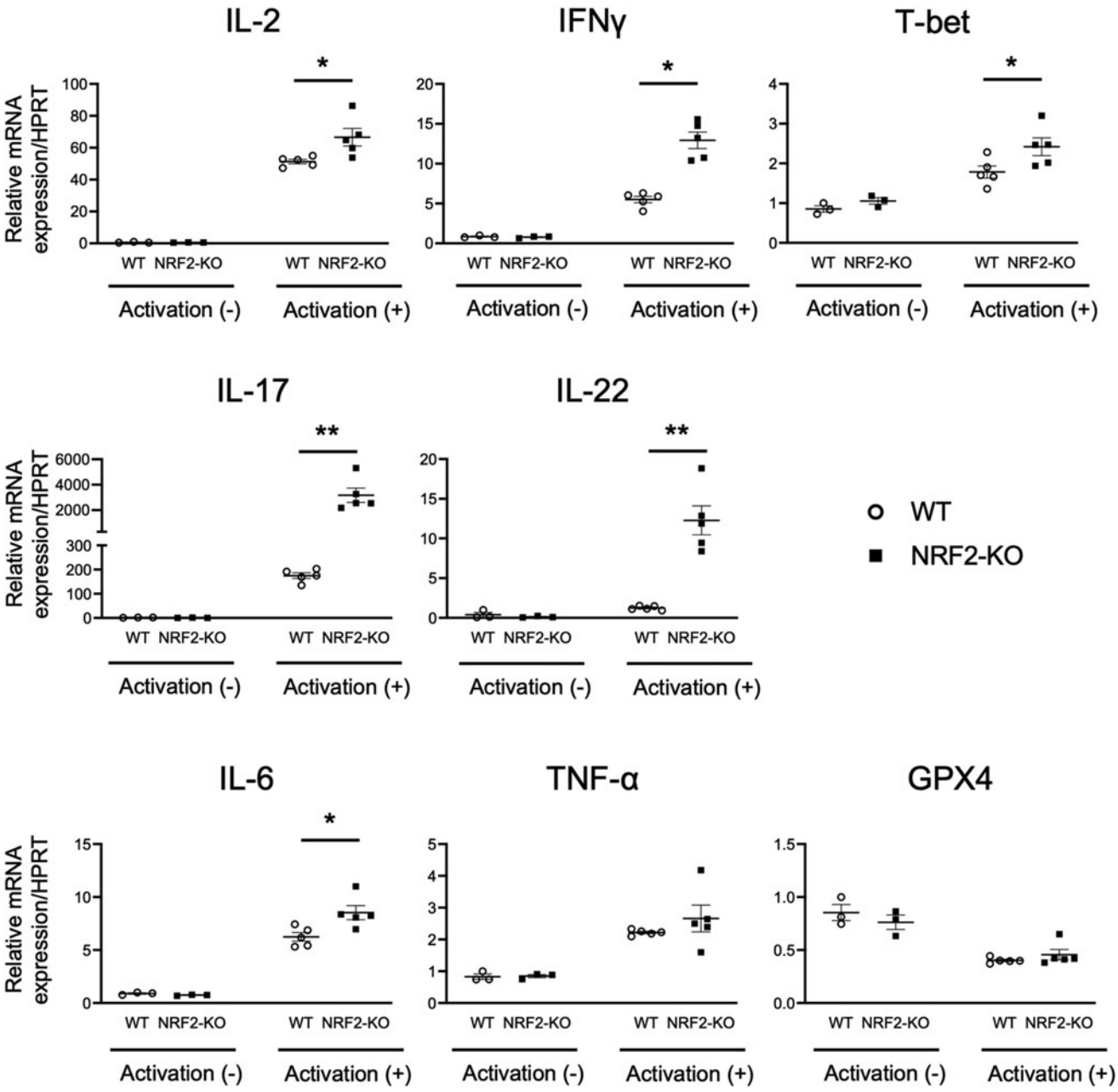

FIG. 3. CD4$^+$ T cell NRF2 signaling suppresses Th1 and Th17 activation *in vitro*. Quantitative RT-PCR-assisted detection of mRNA coding for IL-2, IFNγ, T-bet, IL-17, IL-22, IL-6, TNF-α, and GPX4 in isolated CD4$^+$ T cells before activation ($n=3$ per group) and after activation with anti-CD3/CD28 antibody ($n=5$). The *white circle* indicates WT, and the *black square* indicates NRF2-KO CD4$^+$ T cells. Data are shown as mean $\pm$ SEM. *$p<0.05$, **$p<0.01$, Student's *t*-test. GPX4, glutathione peroxidase 4; T-bet, T-box protein expressed in T cells; TNF-α, tissue necrosis factor-α.

FIG. 4. CD4$^+$ T cell-specific NRF2 signaling mitigates IRI-OLT in the RAG2-KO mouse system. (A) Livers from WT mice subjected to 18 h of cold storage were transplanted into immune-compromised RAG2-KO recipients repopulated with CD4$^+$ T cells (10×10^6 i.v.) from WT *versus* NRF2-KO donor mice and analyzed 6 h post-OLT. **(B)** Representative H&E staining (original magnification $\times$200) and Suzuki's histological grading of liver IRI. **(C)** Representative TUNEL staining and quantification of TUNEL$^+$ cells/HPF. **(D)** Serum AST and ALT levels (U/L). **(E)** Quantitative RT-PCR-assisted detection of mRNA coding for IL-2, IL-17, and IL-6 in OLT. Data were normalized to HPRT gene expression. **(F)** Quantitative RT-PCR-assisted detection of mRNA coding for Foxp3, IL-13, and IL-10 in OLT in RAG2-KO recipients. Data were normalized to HPRT gene expression. The *triangle* indicates untreated RAG2-KO recipient; *white circle* and *black square* indicate RAG2-KO recipient adoptively transferred with CD4$^+$ T cells from WT *versus* NRF2-KO donor mice. Data are shown as mean $\pm$ SEM. $n=4$–6 per each group, *$p<0.05$, **$p<0.01$, ***$p<0.001$, Student's *t*-test.

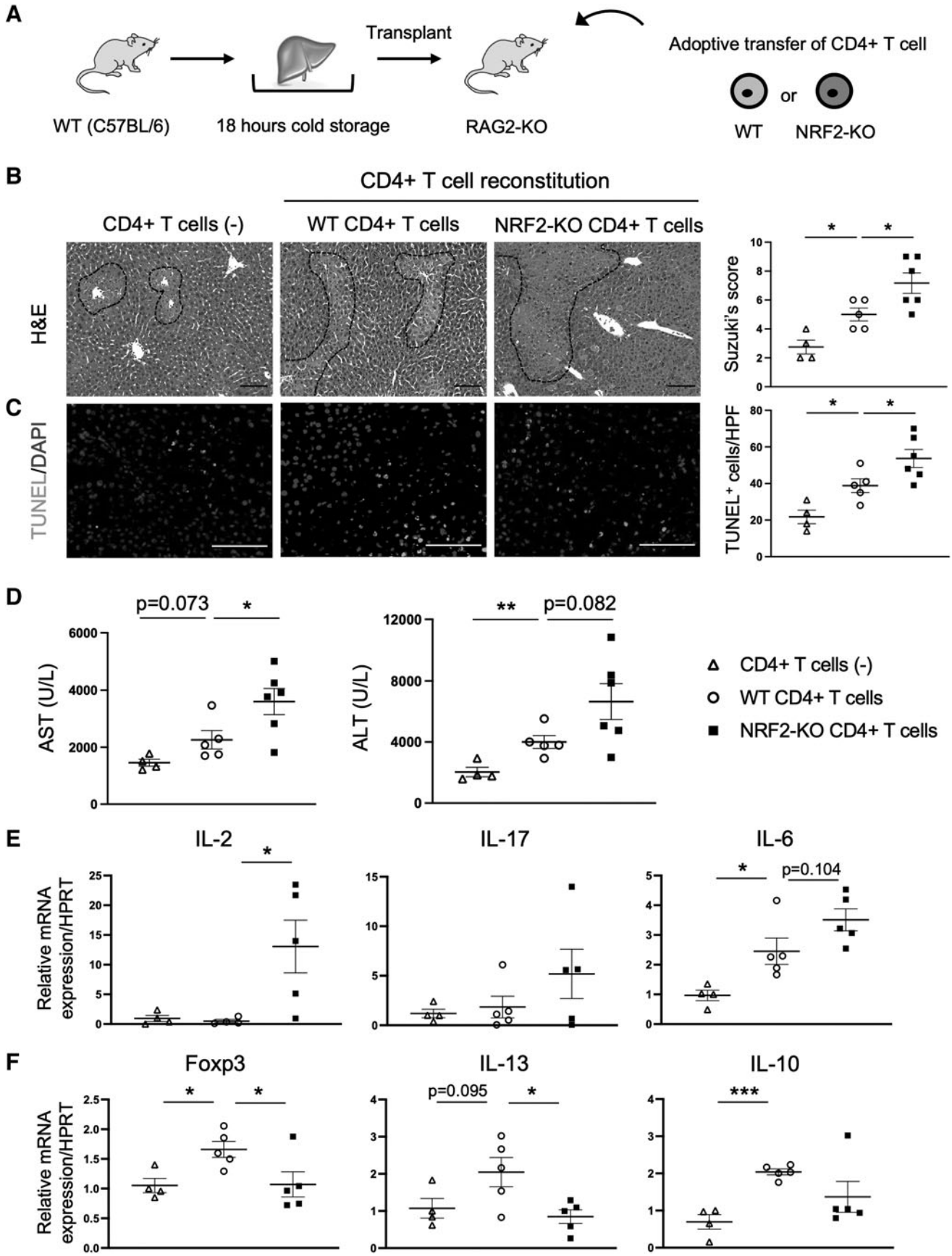
A
Transplant
Adoptive transfer of CD4+ T cell
or
WT (C57BL/6)
18 hours cold storage
RAG2-KO
WT
NRF2-KO
B
CD4+ T cell reconstitution
CD4+ T cells (-)
WT CD4+ T cells
NRF2-KO CD4+ T cells
H&E
Suzuki's score
C
TUNEL/DAPI
TUNEL+ cells/HPF
D
p=0.073
AST (U/L)
ALT (U/L)
p=0.082
CD4+ T cells (-)
WT CD4+ T cells
NRF2-KO CD4+ T cells
E
IL-2
IL-17
IL-6
Relative mRNA expression/HPRT
p=0.104
F
Foxp3
IL-13
IL-10
p=0.095

>95% (Fig. 2A and Supplementary Fig. S1). When we used flow cytometry to evaluate the T cell activation profile, the CD69 expression was significantly lower in $CD4^+$ T cells from WT compared with NRF2-KO mice (WT 6.4% ± 0.3% *vs.* NRF2-KO 8.0% ± 0.4%, $p < 0.05$) (Fig. 2B).

Although the frequency of $CD4^+CD25^+Foxp3^+$ Tregs was comparable in WT and NRF2-KO-naive $CD4^+$ T cells (WT 3.5% ± 0.4% *vs.* NRF2-KO 4.2% ± 0.2%, $p = 0.182$), their numbers significantly increased in stimulated WT compared with NRF2-deficient cultures (WT 15.0% ± 0.5% *vs.* NRF2-KO 11.9% ± 0.4%, $p < 0.01$) (Fig. 2C). Thus, NRF2 signaling promoted $CD4^+$ T cell differentiation into the Treg cell lineage.

$CD4^+$ T cell NRF2 suppresses $CD4^+$ T cell differentiation into the inflammatory phenotype

We then evaluated the T cell cytokine profile by quantitative reverse transcription–polymerase chain reaction (qRT-PCR) in the purified $CD4^+$ T cell cultures. NRF2 knockdown enhanced IL-2, IFNγ, and T-box protein expressed in T cells (T-bet) in stimulated $CD4^+$ T cells ($p < 0.05$, Fig. 3). Furthermore, IL-17 and IL-22 gene expression was enhanced in activated NRF2-deficient compared with WT $CD4^+$ T cells ($p < 0.01$, Fig. 3). In contrast, Th1 and Th17 cytokine expression was comparable in naive unstimulated WT and NRF2-KO $CD4^+$ T cell cultures (IL-2, $p = 0.664$; IFNγ, $p = 0.522$; T-bet, $p = 0.152$; IL-17, $p = 0.073$; IL-22, $p = 0.433$). While IL-6 levels increased in activated NRF2-KO $CD4^+$ T cells (activation–, $p = 0.105$; activation+, $p < 0.05$), there was no significant difference in tissue necrosis factor-α (TNF-α) expression (activation–, $p = 0.857$; activation+, $p = 0.326$) (Fig. 3). Thus, NRF2 signaling suppressed $CD4^+$ T cell differentiation into the proinflammatory phenotype.

Since NRF2-glutathione peroxidase 4 (GPX4) axis might regulate homeostasis by preventing Tregs from lipid peroxidation and ferroptosis (Xu et al, 2021), we assessed its expression in WT and NRF2-KO $CD4^+$ T cell cultures. However, there were no differences in GPX4 signaling between WT and NRF2-deficient $CD4^+$ T cells in naive and activated states (Fig. 3).

$CD4^+$ T cell-specific NRF2 protects mouse liver grafts against IR stress

To elucidate the impact of T cell-specific NRF2 signaling on OLT outcomes, RAG2-KO mice, which do not produce mature T cells or B cells, served as recipients of adoptively transferred purified $CD4^+$ T cells. Such conditioned RAG2-KO mice were then challenged with WT liver grafts, which were subjected to 18 h *ex vivo* cold storage (Fig. 4A). Indeed, adoptive transfer of WT $CD4^+$ T cells increased liver injury in RAG2-KO test recipients, evidenced by histological Suzuki's score (T cell reconstitution −2.8 ± 0.5 *vs.* T cell reconstitution +5.0 ± 0.4, $p < 0.05$), the frequency of $TUNEL^+$ cells (T cell reconstitution −21.8 ± 3.7 cells/HPF *vs.* T cell reconstitution +38.8 ± 3.8 cells/HPF, $p < 0.05$), and serum AST/ALT levels (AST: T cell reconstitution −1456 ± 123 *vs.* T cell reconstitution +2258 ± 322, $p = 0.073$; ALT: T cell reconstitution −2035 ± 306 *vs.* T cell reconstitution +4004 ± 422, $p < 0.01$) (Fig. 4B–D).

In marked contrast, adoptive transfer of NRF2-deficient $CD4^+$ T cells further exacerbated IR-triggered OLT damage in RAG2-KO recipients compared with WT counterparts (NRF2-KO Suzuki's score 7.2 ± 0.7 *vs.* WT, $p < 0.05$; $TUNEL^+$ cells 53.7 ± 4.9 cells/HPF *vs.* WT, $p < 0.05$; AST 3603 ± 460 *vs.* WT, $p < 0.05$; ALT 6649 ± 1174 *vs.* WT, $p = 0.082$) (Fig. 4B–D). Thus, $CD4^+$ T cell-specific NRF2 signaling was required to protect liver grafts from peri-transplant IR stress.

We then analyzed T cell phenotype in WT liver grafts of RAG2-KO recipients repopulated with $CD4^+$ T cells. Indeed, IL-2, IL-17, and IL-6 gene expression increased after transfer of NRF2-deficient compared with NRF2-proficient $CD4^+$ T cells (IL-2, $p < 0.05$; IL-17, $p = 0.255$; IL-6, $p = 0.104$) (Fig. 4E). In parallel, the expression of Foxp3, IL-13, and IL-10 increased after transfer of WT $CD4^+$ T cells compared with untreated RAG2-KO or those repopulated with NRF2-KO $CD4^+$ T cells (no $CD4^+$ T cells *vs.* WT $CD4^+$ T cells and WT $CD4^+$ T cells *vs.* NRF2-KO $CD4^+$ T cells; Foxp3, $p < 0.05$ and $p < 0.05$; IL-13, $p = 0.095$ and $p < 0.05$; IL-10, $p < 0.001$ and $p = 0.152$) (Fig. 4F). Thus, T cell-specific NRF2 signaling was required to promote Treg differentiation and function after transfer into RAG-2 KO mice.

NRF2 negatively regulates proinflammatory phenotype and the hepatocellular injury in human OLT

Having shown the homeostatic function of $CD4^+$ T cell NRF2 signaling in mouse OLT recipients, we next assessed its putative role in a clinical cohort of 45 human liver transplant patients. Donor hepatic biopsies were collected after cold storage before liver implantation, whereas OLT biopsies were sampled at 2 h after portal reperfusion (Fig. 5A). The post-NRF2/pre-NRF2 ratio, reflecting OLT-infiltrating NRF2 immune cells of the recipient origin, negatively correlated with mRNA coding for CD4 ($r = -0.2749$, $p = 0.078$) and CD8 ($r = -0.3252$, $p < 0.05$), indicating that perioperative NRF2 reduced intragraft T cell infiltration.

The post-NRF2/pre-NRF2 ratio also negatively correlated with proinflammatory IL-17 ($r = -0.2997$, $p = 0.054$) and the costimulatory CD28 ($r = -0.3064$, $p < 0.05$) (Fig. 5B). The CD80 and CD86, co-stimulatory innate immune cell ligands for CD28, negatively correlated with the post-NRF2/pre-NRF2 ratio ($r = -0.3355$, $p < 0.05$ and $r = -0.3668$, $p < 0.05$, respectively) (Fig. 5B). Thus, the perioperative NRF2 increase in the human liver grafts was associated with an adaptive suppressive immune signature and a diminished CD80/CD86-CD28 costimulatory phenotype.

TLR4, one of the PRRs that can activate both innate and adaptive immune cells (Palm and Medzhitov, 2009), was also negatively correlated with post-NRF2/pre-NRF2 ratio ($r = -0.3279$, $p < 0.05$) (Fig. 5B). In addition, the post-NRF2/pre-NRF2 ratio negatively correlated with a proinflammatory CXCL10 ($r = -0.2947$, $p = 0.058$) and neutrophil cathepsin G ($r = -0.3250$, $p < 0.05$) (Fig. 5B). Thus, enhanced perioperative NRF2 signaling in human OLT mitigated innate and adaptive immune responses.

To elucidate the influence of perioperative augmented NRF2 signaling on OLT injury, we classified our clinical cohort into post-NRF2/pre-NRF2 ratio ≤1 ($n = 23$) and post-NRF2/pre-NRF2 ratio >1 ($n = 22$) groups. The patient's demographic data and clinical parameters did not reveal significant differences between the groups in OLT recipients or liver donors (Supplementary Table S1A, B). Notably, 51% of OLT recipients failed to increase NRF2 gene expression perioperatively (23 of 45; post-NRF2/pre-NRF2

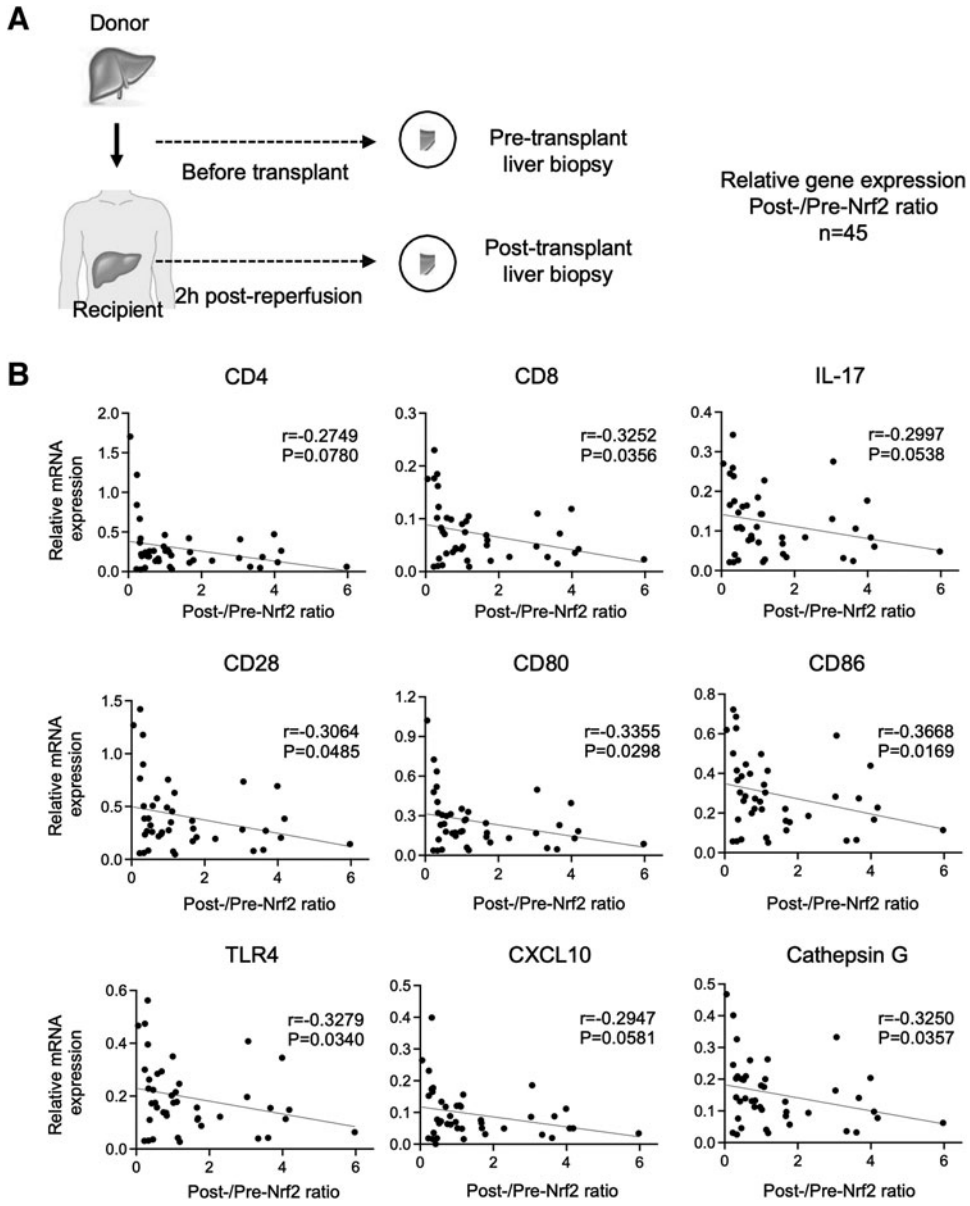

FIG. 5. NRF2 levels in human donor livers negatively correlate with proinflammatory phenotype in OLT patients. (A) Pretransplant (after cold storage) and post-transplant (2 h after portal reperfusion) biopsies were collected from 45 OLT patients. **(B)** Relationship between post-NRF2/pre-NRF2 gene ratio and CD4, CD8, IL-17, CD28, CD80, CD86, TLR4, CXCL10, and cathepsin G gene expressions with β-actin normalization, analyzed by nonparametric Spearman's method. TLR4, Toll-like receptor 4.

ratio ≤1, median 0.998; range, 0.05–5.97) (Supplementary Fig. S2). Although postoperative AST levels were decreased in the patient group with post-NRF2/pre-NRF2 ratio >1 (Fig. 6A), the differences failed to reach statistical significance between the groups on postoperative days (POD) 1–7.

Next, we set the cutoff ratio value of 2 for the perioperative NRF2 increase and classified the 45 patients into post-NRF2/pre-NRF2 ratio ≤2 ($n=35$) and post-NRF2/pre-NRF2 ratio >2 ($n=10$) groups. Although there was a trend of higher donor body mass index ($p=0.065$) and longer warm ischemia time ($p=0.084$) in the group of post-NRF2/pre-NRF2 ratio >2, other demographic variables were comparable between the groups (Supplementary Table S2A, B). Interestingly, compared with the cutoff value of 1, we detected a clearer trend or statistical significance in post-transplant sera AST and ALT levels in the ratio cutoff value of 2 (Fig. 6B), with sera AST (POD 1, $p=0.077$; POD 2, $p=0.046$; POD 3, $p=0.089$; POD 6, $p=0.060$) and ALT (POD 6, $p=0.071$; POD 7, $p=0.046$) levels. Thus, increased perioperative NRF2 signaling is associated with improved hepatoprotection against IR stress in human OLT.

Discussion

The current translational study was designed to elucidate the role of $CD4^+$ T cell NRF2 in IR-stressed OLT. In the experimental arm, we first confirmed that recipient NRF2 signaling was required to mitigate the hepatocellular injury in IR-stressed mouse OLT, whereas adoptive transfer of NRF2-deficient $CD4^+$ T cells into immune-compromised RAG2-KO test mice exacerbated IRI-OLT. Moreover, $CD4^+$ T cell-activated NRF2 suppressed Th1/Th17 while promoting differentiation into $CD4^+CD25^+Foxp3^+$ Treg lineage *in vitro*. In the clinical arm of 45 human OLT patients, the perioperative graft increase of NRF2, derived mainly from host infiltrating immune cells, was negatively associated with Th1/Th17 activation, CD80/CD86-CD28 costimulatory phenotype, and innate immune activation.

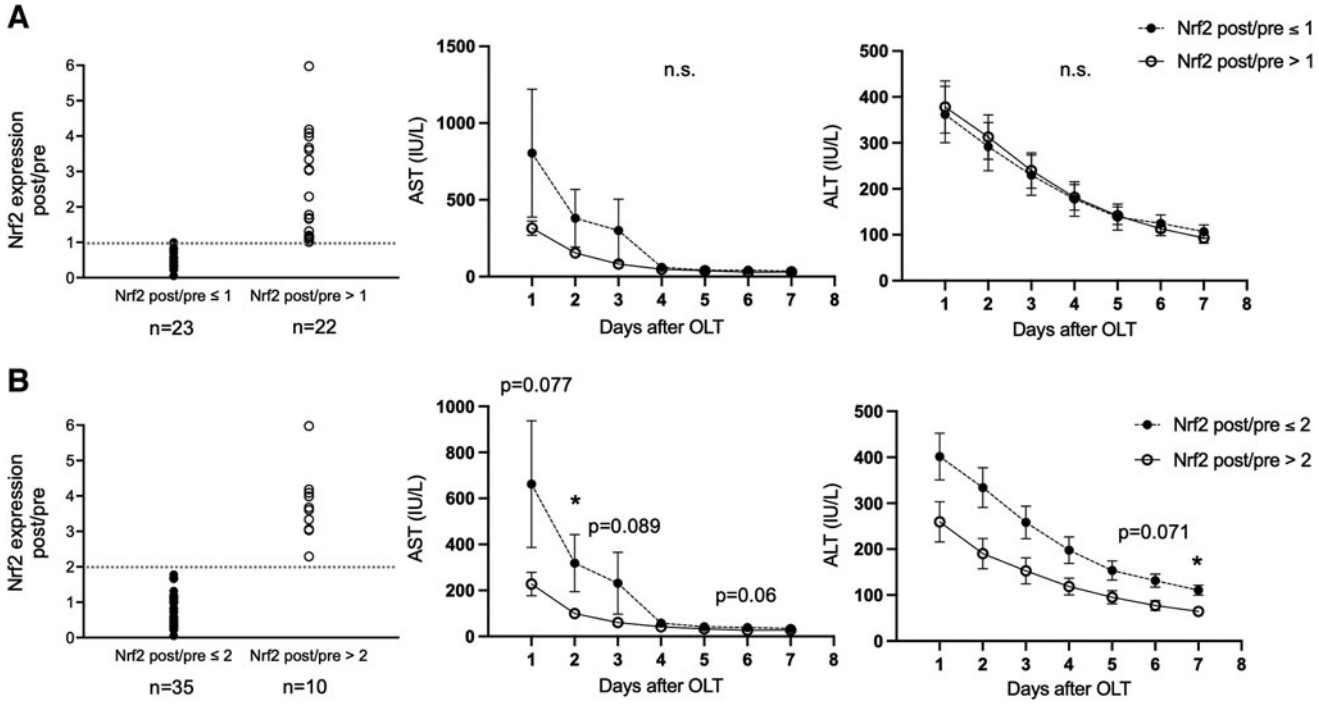

FIG. 6. Increased NRF2 expression in human donor livers attenuates post-transplant OLT injury. (A) Patients were divided into post-NRF2/pre-NRF2 ratio ≤1 ($n = 23$) and post-NRF2/pre-NRF2 ratio >1 ($n = 22$) groups. Serum AST and ALT levels were analyzed at POD 1–7. The *white circle* indicates post-NRF2/pre-NRF2 ratio >1, and the *black circle* indicates post-NRF2/pre-NRF2 ratio ≤1. Data are shown as mean ± SEM. **(B)** Patients were divided into post-NRF2/pre-NRF2 ratio ≤2 ($n = 35$) and post-NRF2/pre-NRF2 ratio >2 ($n = 10$) groups. Serum AST and ALT levels were compared at POD 1–7. The *white circle* indicates post-NRF2/pre-NRF2 ratio >2, and the *black circle* indicates post-NRF2/pre-NRF2 ratio ≤2. Data are shown as mean ± SEM. *$p < 0.05$ (Mann–Whitney U test). POD, postoperative day.

Notably, augmented hepatic NRF2 signaling effectively alleviated the hepatocellular injury in OLT. Although, in addition to CD4$^+$ T cells, other host-derived NRF2 cells may have contributed to intragraft NRF2 signaling, our results highlight the benefit of NRF2 in protecting human OLT. To the best of our knowledge, this study is the first to provide direct evidence that CD4$^+$ T cell-specific NRF2 signaling attenuated IRI-OLT.

The pathogenic role of T cells has been addressed in various solid organ IRI models. The direct evidence is that hepatic and renal IR damage was attenuated in T cell-deficient mice compared with those with an intact immune system, whereas adoptive transfer of T cells restored liver injury (Burne et al, 2001; Zwacka et al, 1997). The relation between T cells and IRI has been confirmed in other solid organ and limb transplant models (Brait et al, 2012; Burne et al, 2001; Rabb et al, 2000; Yilmaz et al, 2006; Zwacka et al, 1997). The suggested mechanisms for CD4$^+$ T cells include secreting cytokines and activating costimulatory molecules to stimulate or inhibit innate immune activation (Rao et al, 2014). Thus, IFNγ and IL-17 promote inflammatory pathology, whereas IL-4, IL-10, and IL-13 mitigate organ IRI.

CD4$^+$ T cells expressing NRF2 represent a promising target to attenuate organ IRI because NRF2 signaling suppresses Th1/Th17 while enhancing Th2/Tregs cells (Suzuki et al, 2020). Indeed, although T cell-specific NRF2 activation by KEAP1 deletion led to the accumulation of intrarenal Tregs and diminished renal damage in mice (Noel et al, 2015), the role of CD4$^+$ T cell-specific NRF2 in the liver IRI has not been studied. This study documents the regulatory function of CD4$^+$ T cell-specific NRF2, both *in vitro* and *in vivo*, suggesting that harnessing NRF2 signaling in CD4$^+$ T cell activation alleviates IRI in OLT recipients.

In a recent study, discarded human liver grafts with increased NRF2 levels showed decreased serum AST, ALT, albumin levels, and a percentage of small droplet macrosteatosis compared with those with lower NRF2 levels (Ahmed et al, 2022). This indicates that NRF2 signaling in hepatocytes, LSECs, and Kupffer cells is essential for homeostatic liver function. A higher post-NRF2/pre-NRF2 ratio in OLT patients was accompanied by somewhat attenuated injury, although the clinical cohort ($n = 35$ *vs.* $n = 10$) was not large enough to show statistical significance (Fig. 6B).

Another clinical study demonstrated that serum NRF2 levels correlated positively with Th2 and negatively with Th1 cytokine programs (Sireesh et al, 2018). While the latter study showed that NRF2 and its downstream targets were decreased in peripheral blood mononuclear cells of diabetes mellitus patients, the precise mechanism by which NRF2 signaling contributes to anti-inflammatory phenotype remains to be elucidated. Our findings provide the proof-of-principle and the rationale to focus on the role of CD4$^+$ T cell NRF2 signaling in post-transplant liver injury in a larger clinical cohort.

In addition to its CD4$^+$ T cell activity, NRF2 directly antagonizes proinflammatory IL-6 and IL-1β and suppresses macrophage inflammatory responses (Kobayashi et al, 2016). NRF2 can also regulate inflammation by exerting antioxidant function and regulating myeloid as well as T cell activation. Our current study extends prior reports on the protective role

of NRF2 in organ IRI (Huang et al, 2014a; Huang et al, 2014b; Ke et al, 2013; Kudoh et al, 2014; Noel et al, 2015; Zhang et al, 2017) by revealing the contribution of $CD4^+$ T cell-specific NRF2 in liver transplants subjected to cold stress. Future studies should clarify cell-specific mechanisms of NRF2 signaling in warm and cold hepatic IRI settings.

Besides the well-known p62-KEAP1-NRF2 axis in the autophagic cell death pathway (Taguchi et al, 2012), much attention has focused on the role of NRF2 in regulated cell death *via* ferroptosis (Dixon et al, 2012), with NRF2 regulating GSH/GPX4 signaling and iron metabolism (Dodson et al, 2019). Although cold stress-induced ferroptosis affects liver IRI (Hattori et al, 2017; Nakamura et al, 2020; Yamada et al, 2020), the expression of GPX4 was comparable in our WT and NRF2-KO $CD4^+$ T cell cultures. Further studies are required to dissect the putative role of NRF2 signaling in the ferroptosis cell death pathway in OLT recipients.

In conclusion, we have documented the essential function of $CD4^+$ T cell-specific NRF2 in hepatic IRI-OLT. Indeed, $CD4^+$ T cell NRF2 signaling inhibited proinflammatory Th1/Th17 cytokines and promoted Treg generation, whereas adoptive transfer of NRF2-enriched $CD4^+$ T cells attenuated IRI-OLT in the RAG2-KO mouse model. In parallel clinical screenings, immune cell NRF2 signaling reduced the hepatic injury in human OLT. These findings provide the rationale for novel strategies targeting $CD4^+$ T cell NRF2 to mitigate organ IRI in transplant recipients.

Materials and Methods

Clinical liver transplant study

This study was approved by the UCLA Institutional Research Board (IRB No. 13-000143). Patients provided informed consent before they participated in the study. We performed a retrospective analysis of 45 adult patients who underwent OLT (May 2013 to August 2015) and received routine standard of care and immunosuppressive therapy. Recipients who underwent re-transplantation were excluded from the study. Donor livers, procured from donation after brain death or cardiac death, were perfused and stored in the University of Wisconsin (UW) solution (Niaspan; Bristol-Myers Squibb, Princeton, NJ). Pretransplant and post-transplant Tru-Cut needle biopsies from the left liver lobe were obtained after cold storage at the back table (before implantation) and about 2 h after portal reperfusion (before abdominal closure). Hepatic biopsies were screened by qRT-PCR with β-actin normalization for NRF2, CD4, CD8, IL-17, CD28, CD80, CD86, TLR4, CXCL10, and cathepsin G. Recipient blood was collected before the transplant and at POD 1–7. Liver injury was evaluated with serum AST and ALT.

Animals

WT, RAG2-KO, and NRF2-KO mice (C57BL/6) were purchased from the Jackson Laboratory and used at 8–10 weeks of age. Animals were housed in the UCLA animal facility under specific pathogen-free conditions and received humane care according to the criteria outlined in the Guide for the Care and Use of Laboratory Animals (National Academies Press, 2011). Their use was approved by UCLA Animal Research Committee (ARC No. 1999-094).

Mouse OLT model

We used a mouse model of *ex vivo* cold hepatic storage followed by OLT, as described by our group (Kageyama et al, 2018b). To mimic the marginal human OLT setting, donor livers were stored in the UW solution at 4°C for 18 h before transplantation. Liver graft and serum samples were collected 6 h after reperfusion, the peak of hepatocellular damage in this model. The sham group underwent the same procedures except for OLT.

Adoptive transfer of $CD4^+$ T cells

Syngeneic spleen $CD4^+$ T cells, separated from groups of WT or NRF2-KO mice by magnetic cell sorting kit (EasySep Mouse $CD4^+$ T Cell Isolation Kit; StemCell Technologies, Vancouver, Canada), were adoptively transferred (1×10^7 i.v.), into RAG2-KO mice, in which T and B cells are absent. These animals were subjected to OLT 1 h after the adoptive transfer.

Liver enzyme assay

Serum AST/ALT levels were measured with AST/ALT Liquid Reagent Kit (Teco Diagnostics) and validated with Validate GC3 (Maine Standards Company, LLC).

OLT histology and IRI grading

Formalin-fixed paraffin-embedded liver sections (4 μm) were stained with hematoxylin and eosin staining. The severity of IRI was graded using Suzuki's criteria (Suzuki et al, 1993).

TUNEL assay

Cell death in liver sections (4 μm) was detected by *In Situ* Apoptosis Detection Kit (Clontech) according to the manufacturer's protocol. Results were scored semiquantitatively by blindly counting the number of positive cells in 10 HPF/section.

$CD4^+$ T cell isolation and culture

Spleens resected from WT or NRF2-KO were passed through a 70 μm strainer and washed with sterile PBS. After lysing red blood cells, $CD4^+$ T cells were purified with a negative selection (EasySep Mouse $CD4^+$ T Cell Isolation Kit). Isolated $CD4^+$ T cells were plated at a concentration of 1×10^6/mL in six-well plates that were precoated with 5 μg/mL anti-CD3e (clone: 145-2C11; eBioscience, San Diego, CA) and cultured in RPMI 1640 in the presence of 5 μg/mL anti-CD28 (clone: 37.51; eBioscience) and supplemented with 10% fetal bovine serum, 100 U/mL penicillin and 100 μg/mL streptomycin, 10 m*M* 4-(2-hydroxyethyl)-1-piperazineethanesulfonic acid (HEPES), 2 m*M* L-glutamine, and non-essential amino acids at 37°C in a humidified atmosphere incubator containing 5% CO_2 for 48 h.

qRT-PCR analysis

RNA extracted with the RNAse Mini Kit (Qiagen) was reverse-transcribed into complementary DNA (cDNA). Quantitative PCR was performed using QuantStudio 3 (Applied Biosystems). The primer sequences are listed in

Supplementary Table S3. The expression of the target gene was normalized to the housekeeping β-actin or HPRT.

Immunofluorescence

Mouse liver samples were stained with rabbit anti-CD68 antibody (Abcam) and rat anti-Ly6G antibody (BD Biosciences, San Jose, CA). Signals were visualized with secondary Alexa Fluor antibodies (Invitrogen, Thermo Fisher Scientific). Hepatic CD68$^+$ and Ly6G$^+$ cells were scored semiquantitatively by counting cells in 10 HPF/section ($\times$400).

Flow cytometry

Isolated CD4$^+$ T cells were incubated with anti-mouse CD16/32 antibody (clone: 93; BioLegend, San Diego, CA) to block Fc-mediated nonspecific antibody binding. Cells were then stained with the fluorochrome-conjugated antibodies; CD4-APC (clone: RM4-5;100515; BioLegend), CD69-FITC (clone: H1.2F3;104506; BioLegend), and the antibodies in the True-Nuclear Mouse Treg Flow Kit (320029; BioLegend). Multi-parameter flow cytometric analysis was performed using an LSRFortessa X-20 SORP (BD Biosciences), and results were analyzed using BD FACSDiva software (BD Biosciences) at the UCLA Jonsson Comprehensive Cancer Center (JCCC) and Center for AIDS Research Flow Cytometry Core Facility (UCLA).

Statistics

For human data, continuous values were analyzed by the Mann–Whitney *U* test and categorical variables by Fisher's exact test. Spearman's correlation coefficient (r) was used to evaluate the strength of the linear relationship between variables. For mouse experiments, comparisons between the two groups were assessed using a Student's *t*-test. All p values were two-tailed, and $p < 0.05$ was considered statistically significant. GraphPad Prism 9 was used for statistical analyses.

Acknowledgments

We thank Ko Takanashi and Christopher Creencia (UCLA—Translational Pathology Core Laboratory) for immunohistochemical stain assistance.

Authors' Contributions

H.K., K.K., and J.W.K.-W.: study concept/design. H.K., K.K., H.H., and K.J.D.: experimental data acquisition. H.K.: surgical procedures. H.K. and K.K.: data analyses. H.K., K.K., and J.W.K.-W.: drafted article. J.W.K.-W.: obtained funding. All authors have read/edited the article.

Author Disclosure Statement

The authors declare that they have no conflict of interest.

Funding Information

This study was supported by the National Institutes of Health Grants: P01 AI120944, R01 DK062357, R01 DK107533, and R01 DK102110 (J.W.K.-W.).

Supplementary Material

Supplementary Table S1
Supplementary Table S2
Supplementary Table S3
Supplementary Figure S1
Supplementary Figure S2

References

Ahmed O, Xu M, Zhou F, et al. NRF2 assessment in discarded liver allografts: A role in allograft function and salvage. Am J Transplant 2022;22(1):58–70; doi: 10.1111/ajt.16789

Brait VH, Arumugam TV, Drummond GR, et al. Importance of T lymphocytes in brain injury, immunodeficiency, and recovery after cerebral ischemia. J Cereb Blood Flow Metab 2012;32(4):598–611; doi: 10.1038/jcbfm.2012.6

Burne MJ, Daniels F, El Ghandour A, et al. Identification of the CD4(+) T cell as a major pathogenic factor in ischemic acute renal failure. J Clin Invest 2001;108(9):1283–1290; doi: 10.1172/JCI12080

Chen D, Tavana O, Gu W. ARF-NRF2: A new checkpoint for oxidative stress responses? Mol Cell Oncol 2018;5(3): e1432256; doi: 10.1080/23723556.2018.1432256

Cong P, Liu Y, Liu N, et al. Cold exposure induced oxidative stress and apoptosis in the myocardium by inhibiting the Nrf2-Keap1 signaling pathway. BMC Cardiovasc Disord 2018;18(1):36; doi: 10.1186/s12872-018-0748-x

Dixon SJ, Lemberg KM, Lamprecht MR, et al. Ferroptosis: An iron-dependent form of nonapoptotic cell death. Cell 2012; 149(5):1060–1072; doi: 10.1016/j.cell.2012.03.042

Dodson M, Castro-Portuguez R, Zhang DD. NRF2 plays a critical role in mitigating lipid peroxidation and ferroptosis. Redox Biol 2019;23:101107; doi: 10.1016/j.redox.2019 .101107

Galicia-Moreno M, Lucano-Landeros S, Monroy-Ramirez HC, et al. Roles of Nrf2 in liver diseases: Molecular, pharmacological, and epigenetic aspects. Antioxidants (Basel) 2020; 9(10):980; doi: 10.3390/antiox9100980

Guo J, Hu H, Chen Z, et al. Cold exposure induces intestinal barrier damage and endoplasmic reticulum stress in the colon via the SIRT1/Nrf2 signaling pathway. Front Physiol 2022; 13:822348; doi: 10.3389/fphys.2022.822348

Hattori K, Ishikawa H, Sakauchi C, et al. Cold stress-induced ferroptosis involves the ASK1–p38 pathway. EMBO Rep 2017;18:2067–2078; doi: 10.15252/embr.201744228

Hayes JD, Dinkova-Kostova AT. The Nrf2 regulatory network provides an interface between redox and intermediary metabolism. Trends Biochem Sci 2014;39:199–218; doi: 10.1016/j.tibs.2014.02.002

Huang J, Shen XD, Yue S, et al. Adoptive transfer of heme oxygenase-1 (HO-1)-modified macrophages rescues the nuclear factor erythroid 2-related factor (Nrf2) antiinflammatory phenotype in liver ischemia/reperfusion injury. Mol Med 2014a;20:448–455; doi: 10.2119/molmed.2014 .00103

Huang J, Yue S, Ke B, et al. Nuclear factor erythroid 2-related factor 2 regulates toll-like receptor 4 innate responses in mouse liver ischemia-reperfusion injury through Akt-forkhead box protein O1 signaling network. Transplantation 2014b;98:721–728; doi: 10.1097/TP.0000000000000316

Kageyama S, Kadono K, Hirao H, et al. Ischemia-reperfusion injury in allogeneic liver transplantation: A role of CD4 T cells in early allograft injury. Transplantation 2021;105: 1989–1997; doi: 10.1097/TP.0000000000003488

Kageyama S, Nakamura K, Fujii T, et al. Recombinant relaxin protects liver transplants from ischemia damage by hepatocyte glucocorticoid receptor: From bench-to-bedside. Hepatology 2018a;68:258–273; doi: 10.1002/hep.29787

Kageyama S, Nakamura K, Ke B, et al. Serelaxin induces Notch1 signaling and alleviates hepatocellular damage in orthotopic liver transplantation. Am J Transplant 2018b;18: 1755–1763; doi: 10.1111/ajt.14706

Ke B, Shen XD, Zhang Y, et al. KEAP1-NRF2 complex in ischemia-induced hepatocellular damage of mouse liver transplants. J Hepatol 2013;59:1200–1207; doi: 10.1016/j.jhep.2013.07.016

Kobayashi EH, Suzuki T, Funayama R, et al. Nrf2 suppresses macrophage inflammatory response by blocking proinflammatory cytokine transcription. Nat Commun 2016;7: 11624; doi: 10.1038/ncomms11624

Kudoh K, Uchinami H, Yoshioka M, et al. Nrf2 activation protects the liver from ischemia/reperfusion injury in mice. Ann Surg 2014;260:118–127; doi: 10.1097/SLA.0000000000000287

Liu Y, Ji H, Zhang Y, et al. Negative $CD4^+$ TIM-3 signaling confers resistance against cold preservation damage in mouse liver transplantation. Am J Transplant 2015;15:954–964; doi: 10.1111/ajt.13067

Nakamura K, Kageyama S, Kaldas FM, et al. Hepatic CEACAM1 expression indicates donor liver quality and prevents early transplantation injury. J Clin Invest 2020;130:2689–2704; doi: 10.1172/JCI133142

National Research Council. Guide for the care and use of laboratory animals. Eighth edition. The National Academies Press: Washington, DC; 2011.

Noel S, Martina MN, Bandapalle S, et al. T lymphocyte-specific activation of Nrf2 protects from AKI. J Am Soc Nephrol 2015;26:2989–3000; doi: 10.1681/ASN.2014100978

Oshi M, Angarita FA, Tokumaru Y, et al. High expression of NRF2 is associated with increased tumor-infiltrating lymphocytes and cancer immunity in ER-positive/HER2-negative breast cancer. Cancers (Basel) 2020;12:3856; doi: 10.3390/cancers12123856

Palm NW, Medzhitov R. Pattern recognition receptors and control of adaptive immunity. Immunol Rev 2009;227:221–233; doi: 10.1111/j.1600-065X.2008.00731.x

Rabb H, Daniels F, O'Donnell M, et al. Pathophysiological role of T lymphocytes in renal ischemia-reperfusion injury in mice. Am J Physiol Renal Physiol 2000;279:F525–F531; doi: 10.1152/ajprenal.2000.279.3.F525

Rao J, Lu L, Zhai Y. T cells in organ ischemia reperfusion injury. Curr Opin Organ Transplant 2014;19:115–120; doi: 10.1097/MOT.0000000000000064

Rockwell CE, Zhang M, Fields PE, et al. Th2 skewing by activation of Nrf2 in CD4(+) T cells. J Immunol 2012;188: 1630–1637; doi: 10.4049/jimmunol.1101712

Sireesh D, Dhamodharan U, Ezhilarasi K, et al. Association of NF-E2 related factor 2 (Nrf2) and inflammatory cytokines in recent onset type 2 diabetes mellitus. Sci Rep 2018;8(1): 5126; doi: 10.1038/s41598-018-22913-6

Suzuki S, Toledo-Pereyra LH, Rodriguez FJ, et al. Neutrophil infiltration as an important factor in liver ischemia and reperfusion injury. Modulating effects of FK506 and cyclosporine. Transplantation 1993;55(6):1265–1272; doi: 10.1097/00007890-199306000-00011

Suzuki T, Hidaka T, Kumagai Y, et al. Environmental pollutants and the immune response. Nat Immunol 2020;21(12): 1486–1495; doi: 10.1038/s41590-020-0802-6

Taguchi K, Fujikawa N, Komatsu M, et al. Keap1 degradation by autophagy for the maintenance of redox homeostasis. Proc Natl Acad Sci U S A 2012;109(34):13561–13566; doi: 10.1073/pnas.1121572109

Tonelli C, Chio IIC, Tuveson DA. Transcriptional regulation by Nrf2. Antioxid Redox Signal 2018;29(17):1727–1745; doi: 10.1089/ars.2017.7342

Tsung A, Hoffman RA, Izuishi K, et al. Hepatic ischemia/reperfusion injury involves functional TLR4 signaling in nonparenchymal cells. J Immunol 2005;175(11):7661–7668; doi: 10.4049/jimmunol.175.11.7661

Turley AE, Zagorski JW, Rockwell CE. The Nrf2 activator tBHQ inhibits T cell activation of primary human CD4 T cells. Cytokine 2015;71(2):289–295; doi: 10.1016/j.cyto.2014.11.006

Xu C, Sun S, Johnson T, et al. The glutathione peroxidase Gpx4 prevents lipid peroxidation and ferroptosis to sustain Treg cell activation and suppression of antitumor immunity. Cell Rep 2021;35(11):109235; doi: 10.1016/j.celrep.2021.109235

Yamada N, Karasawa T, Wakiya T, et al. Iron overload as a risk factor for hepatic ischemia-reperfusion injury in liver transplantation: Potential role of ferroptosis. Am J Transplant 2020;20(6):1606–1618; doi: 10.1111/ajt.15773

Yilmaz G, Arumugam TV, Stokes KY, et al. Role of T lymphocytes and interferon-gamma in ischemic stroke. Circulation 2006;113(17):2105–2112; doi: 10.1161/CIRCULATIONAHA.105.593046

Zhai Y, Petrowsky H, Hong JC, et al. Ischaemia-reperfusion injury in liver transplantation—From bench to bedside. Nat Rev Gastroenterol Hepatol 2013;10(2):79–89; doi: 10.1038/nrgastro.2012.225

Zhai Y, Shen XD, O'Connell R, et al. Cutting edge: TLR4 activation mediates liver ischemia/reperfusion inflammatory response via IFN regulatory factor 3-dependent MyD88-independent pathway. J Immunol 2004;173(12):7115–7119; doi: 10.4049/jimmunol.173.12.7115

Zhang C, Zhang Y, Liu Y, et al. A soluble form of P selectin glycoprotein ligand 1 requires signaling by nuclear factor erythroid 2-related factor 2 to protect liver transplant endothelial cells against ischemia-reperfusion injury. Am J Transplant 2017;17(6):1462–1475; doi: 10.1111/ajt.14159

Zhao M, Chen H, Ding Q, et al. Nuclear factor erythroid 2-related factor 2 deficiency exacerbates lupus nephritis in B6/lpr mice by regulating Th17 cell function. Sci Rep 2016;6: 38619; doi: 10.1038/srep38619

Zwacka RM, Zhang Y, Halldorson J, et al. CD4(+) T-lymphocytes mediate ischemia/reperfusion-induced inflammatory responses in mouse liver. J Clin Invest 1997; 100(2):279–289; doi: 10.1172/JCI119533

Address correspondence to:
Prof. Jerzy W. Kupiec-Weglinski
The Dumont-UCLA Transplantation Center
Department of Surgery
Division of Liver and Pancreas Transplantation
David Geffen School of Medicine at UCLA
77-120 CHS, 10833 Le Conte Avenue
Los Angeles, CA 90095
USA

E-mail: jkupiec@mednet.ucla.edu

Date of first submission to ARS Central, July 18, 2022; date of acceptance, September 5, 2022.

Abbreviations Used

ALT = alanine aminotransferase
AST = aspartate aminotransferase
GPX4 = glutathione peroxidase 4
GSH = glutathione
H&E = hematoxylin and eosin
HPF = high-power field
IR = ischemia and reperfusion
IRI = ischemia–reperfusion injury
LAG3 = lymphocyte activation gene 3
LSECs = liver sinusoidal endothelial cells
mRNA = messenger RNA
NRF2 = nuclear factor erythroid 2-related factor 2
OLT = orthotopic liver transplantation
PD-1 = programmed death-1
POD = postoperative day
PRRs = pattern recognition receptors
qRT-PCR = quantitative reverse transcription–polymerase chain reaction
RT-PCR = reverse transcription–polymerase chain reaction
SEM = standard error of the mean
T-bet = T-box protein expressed in T cells
TIM-3 = T cell immunoglobulin and mucin-domain containing-3
TLR4 = Toll-like receptor 4
TNF-α = tissue necrosis factor-α
Tregs = regulatory T cells
TUNEL = TdT-mediated dUTP nick end labeling
UW = University of Wisconsin
WT = wild type